Numerical tests of nucleation theories for the Ising models

Seunghwa Ryu[1] and Wei Cai[2]
[1]*Department of Physics, Stanford University, Stanford, California 94305, USA*
[2]*Department of Mechanical Engineering, Stanford University, Stanford, California 94305, USA*
(Received 11 April 2010; revised manuscript received 21 June 2010; published 15 July 2010)

The classical nucleation theory (CNT) is tested systematically by computer simulations of the two-dimensional (2D) and three-dimensional (3D) Ising models with a Glauber-type spin flip dynamics. While previous studies suggested potential problems with CNT, our numerical results show that the fundamental assumption of CNT is correct. In particular, the Becker-Döring theory accurately predicts the nucleation rate if the correct droplet free energy function is provided as input. This validates the coarse graining of the system into a one dimensional Markov chain with the largest droplet size as the reaction coordinate. Furthermore, in the 2D Ising model, the droplet free energy predicted by CNT matches numerical results very well, after a logarithmic correction term from Langer's field theory and a constant correction term are added. But significant discrepancies are found between the numerical results and existing theories on the magnitude of the logarithmic correction term in the 3D Ising model. Our analysis underscores the importance of correctly accounting for the temperature dependence of surface energy when comparing numerical results and nucleation theories.

DOI: 10.1103/PhysRevE.82.011603 PACS number(s): 64.60.qe, 64.60.My, 05.50.+q

I. INTRODUCTION

Nucleations are ubiquitously observed in many different systems including supercooled fluids [1–3], nanomaterials [4], polymerization processes [5], and electro-weak phase transitions [6]. The standard theory used to describe the nucleation phenomena is the classical nucleation theory (CNT) [7–10]. CNT considers the droplets of the stable phase spontaneously formed in the background of the metastable phase. The maximum in the droplet free energy as a function of droplet size is the free energy barrier of nucleation, and is the dominant factor in the determination of the nucleation rate. A widely used form of CNT is the Becker-Döring theory [7] that predicts the nucleation rate from a steady-state solution of a one-dimensional (1D) Markov chain model.

While CNT successfully captures many qualitative features of nucleation events, the prediction of the nucleation rate based on CNT cannot be compared quantitatively with experiments [11], given the gross approximations made in the theory. During the past 50 years, many modifications and extensions of CNT have been developed. For example, Lothe and Pound [12] considered the contributions from extra degrees of freedom of a cluster (in addition to its size) to its Gibbs free energy of formation. Langer [13,14] developed a field theory to extend the Becker-Döring steady-state solution to include the effect of other microscopic degrees of freedom of a cluster. Zeng and Oxtoby [15] improved the temperature dependence of the nucleation rate predicted by CNT by expressing the droplet free energy as a functional of the radial density profile $\rho(r)$. To date, many nucleation theories have been developed, but it is very difficult to verify them experimentally, due to the difficulties in measuring nucleation rates accurately. While for a theory, it is more convenient to study homogeneous nucleations in a single-component system, such conditions are difficult to achieve in experiments [11]. Instead, experimental measurements are usually influenced by surface structures and impurities that are difficult to control.

Computer simulations have the opportunity to probe nucleation processes in great detail and to quantitatively check the individual components of the nucleation theories. The increase of computational power and the development of advanced sampling algorithms allow the calculation of nucleation rates for model systems over a wide range of conditions [16–19]. A prototypical nucleation problem is the decay of the magnetization in the two-dimensional (2D) or three-dimensional (3D) Ising model, which has been studied by computer simulations for several decades [20–30]. Both agreement [22,28,29] and disagreement [20,21,25,30] between numerical results and CNT predictions have been reported.

When the CNT predictions of nucleation rate do not agree with numerical results, several potential problems of CNT were usually discussed. For example, a suspect is the application of surface tension of macroscopic, flat, interfaces to a small droplet [21]. The validity of coarse graining the many-spin system into a one-dimensional Markov chain was also questioned [21,25]. Nucleation theories usually express the rate in the Arrhenius form, with a free-energy barrier and a pre-exponential factor. Usually both terms are not computed in the same study. Hence, we often cannot conclude which one causes the discrepancy between CNT and numerical simulations, and how the theory should be improved. Only rarely did numerical results lead to clear conclusions on the validity of the fundamental assumptions made in CNT [27].

In a recent communication [31], we presented numerical results that systematically test the different parts of the Becker-Döring theory, as applied to 2D and 3D Ising models. The purpose of this paper is to provide a more in-depth discussion of these tests, and to present results that were omitted due to space constraints. We compute the nucleation rate by the forward flux sampling (FFS) method [32], which allows the rate to be calculated over a much wider range of external field and temperature conditions than that possible by brute force Monte Carlo simulations. To test the individual components of CNT (Becker-Döring theory), the free energy $F(n)$ of the droplet as a function of droplet size n is

computed using the umbrella sampling method [18]. The kinetic prefactor of the critical cluster, f_c^+, which is part of the Becker-Döring theory, is computed independently from Monte Carlo simulations starting from the ensemble of critical clusters. The nucleation rate predicted by the Becker-Döring theory, using the so computed $F(n)$ and f_c^+ as inputs, is compared with the nucleation rate directly computed from the FFS method.

We find that, provided with the correct droplet free energy $F(n)$, the Becker-Döring theory predicts the nucleation rate very accurately. This confirms that the coarse-graining of the Ising model as a one-dimensional Markov chain, as invoked in CNT, is a very good approximation, which was also noted earlier [24,27]. Discrepancies between the droplet free energy $F(n)$ predicted by CNT and numerical results have been reported earlier [24,25]. Here, we show that if a logarithmic correction term and a constant correction term are added, the theoretical prediction of droplet free energy agrees very well with the numerical result. The logarithmic correction term was first derived from Langer's field theory, but was customarily put as a correction to the kinetic prefactor. Our analysis shows that this correction term should be placed in the free energy function $F(n)$ in order to correctly predict the size of the critical nucleus. In 2D both the logarithmic correction term and the constant term can be determined from existing analytic expressions and hence contain no fitting parameters. On the other hand, in 3D both the coefficient of the logarithmic correction term and the constant term need to be treated as fitting parameters in this work.

Our analysis resolved some of the previously reported discrepancies between numerical simulations and CNT. For the 2D Ising model, the logarithmic correction term to the droplet free energy was often neglected [21,24]. Because the logarithmic correction term is positive and substantial in 2D, the omission of this term would cause CNT to grossly overestimate the nucleation rate. For the 3D Ising model, the logarithmic correction term is much smaller relative to the other terms. However, the temperature dependence of the surface free energy was sometimes ignored [25,30]. While the surface free energy can be approximated as a constant at very low temperatures [28], it decreases appreciably with temperature above a quarter of the critical temperature. Overestimating the surface free energy would lead to an overestimate of the nucleation barrier and an underestimate of the nucleation rate.

The paper is organized as follows. Section II summarizes a number of nucleation theories and their applications to the 2D and 3D Ising model. Section III presents the numerical methods we employ to test these theories. The numerical results are compared with the nucleation theories in Sec. IV. A brief summary is given in Sec. V.

II. NUCLEATION THEORIES

A. Brief review of nucleation theories

In 1926, Volmer and Weber [33] first introduced the concept of critical droplet and estimated the nucleation rate in a supersaturated vapor by the following equation,

$$I \approx f_c^+ \exp\left(-\frac{F_c}{k_B T}\right), \tag{1}$$

where F_c is the formation free energy of the critical droplet, and f_c^+ is the attachment rate of molecules to the critical droplet. F_c is the maximum of the droplet free energy as a function of droplet size n. The Volmer-Weber theory also gives the droplet free energy function in the following form,

$$F(n) = \sigma S - \delta\mu n, \tag{2}$$

where σ is the effective surface tension and S is surface area. $\delta\mu$ is the bulk chemical potential difference per molecule between the liquid and the vapor phases. n is the total number of molecules in the droplet. The concepts of critical droplet, its free energy, and the attachment rate of molecules, still remain important to date for our understanding of the nucleation process. Other dynamical factors, such as multiple recrossing of the free-energy barrier, originally ignored in the Volmer-Weber theory, were recognized later.

In 1935, Becker and Döring [7] modeled the time evolution of the droplet population using a one-dimensional Markov chain model [10], and obtained a steady-state solution for the nucleation rate. This solution finally pinpoints the kinetic prefactor [51] in the nucleation rate, which is expressed as

$$I = f_c^+ \Gamma \exp\left(-\frac{F_c}{k_B T}\right), \tag{3}$$

where Γ is known as the Zeldovich factor [8,9] defined by

$$\Gamma \equiv \left(\frac{\eta}{2\pi k_B T}\right)^{1/2}, \quad \eta = -\left.\frac{\partial^2 F(n)}{\partial n^2}\right|_{n=n_c}. \tag{4}$$

The flatter is the free-energy curve near the critical size n_c, the smaller is the Zeldovich factor. For two systems having the same free-energy barriers, the system with the flatter free energy landscape near the barrier has more diffusive nucleation dynamics and its nucleation rate is lower. Hence, the Zeldovich factor captures the multiple recrossing of the free energy barrier. A systematic investigation of the relation between the Zeldovich factor and recrossing can be found in Pan and Chandler [25].

There are two fundamental assumptions in CNT that are independent of each other. First, the time evolution of the droplet population can be described by a 1D Markov chain model. Second, the free energy of a droplet can be written as Eq. (2), where σ is the surface tension of macroscopic interfaces. We can test the first assumption if we can compute the nucleation rate using a numerical method that does not rely on the Markovian assumption. We can test the second assumption by computing the free energy function by umbrella sampling.

In 1967, Langer [14] developed a field theoretical approach to take into account all degrees of freedom of a droplet when calculating the steady-state solution for the nucleation rate. This is a generalization of the Becker-Döring theory to incorporate microscopic (fluctuation) degrees of freedom of the droplet. Langer's field theory was later used to derive a correction term to the nucleation rate in the drop-

let model [34–37]. In the literature, the field theory correction is usually expressed as an extra term in the preexponential factor in Eq. (3). But it can also be expressed as a modification to the free energy function in Eq. (2), changing it to

$$F(n) = \sigma S - \delta\mu n + \tau k_B T \ln n. \tag{5}$$

While both approaches can give rise to similar predictions to the nucleation rate, we will show later that it is more self-consistent to include the correction term in the free energy.

The field theory predicts that, for an isotropic medium, the coefficient of logarithmic correction term is $\tau=\frac{5}{4}$ in 2D [38] and $\tau=-\frac{1}{9}$ in 3D [39]. However, it was later predicted that the shape fluctuation of a 3D droplet should be suppressed below the roughening temperature [37], which leads to $\tau=-\frac{2}{3}$. Our numerical results confirm the $\tau=\frac{5}{4}$ prediction for the 2D Ising model, under a wide range of temperatures. This contradicts an earlier numerical study [21] which suggests that τ is close to zero at low temperatures and only rise to $\frac{5}{4}$ at high temperatures. On the other hand, our numerical results are not consistent with any of the above theoretical predictions of τ for the 3D Ising model. This problem may be related to the finding by Zia and Wallace [40], that the excitation spectrum around a 3D droplet is affected by the anisotropy of the medium, but that around a 2D droplet is not affected by anisotropy. Because the Ising model is fundamentally anisotropic (e.g., with cubic symmetry), the field theoretic prediction based on isotropic medium may not apply to the 3D Ising model.

All the nucleation theories mentioned above share several fundamental assumptions: (1) only isolated droplets are considered and the interaction between droplets is neglected; (2) a droplet is assumed to be compact with a well-defined surface; (3) the surface energy expression derived from a macroscopically planar surface can be applied to the surface of a very small droplet. The first two assumptions are valid at temperatures much lower than the critical temperature and at small magnetic field. Under these conditions, the density of droplets is very small and each droplet tends to be compact [52]. We will not test these two assumptions in this study. In other words, our numerical simulations will be limited to the low temperature and small field conditions where these assumptions should be valid. Models that account for droplet interactions exist in the literature [41] but will not be discussed in this paper.

Even with the logarithmic correction term, Eq. (5) still deviates from the numerically computed droplet free energy (from umbrella sampling) by a constant. This constant term is likely to be caused by the third assumption listed above. We found that in the 2D Ising model this discrepancy can be removed by adding a constant term to the droplet free energy

$$F(n) = \sigma S - \delta\mu n + \tau k_B T \ln n + d(T). \tag{6}$$

In 2D, the constant term d can be determined without any fitting to the numerical results. At each temperature T, d can be obtained by matching $F(n)$ with analytic expressions of droplet free energy that are available for very small droplets [21] (Appendix D). Unfortunately, in 3D even Eq. (6) does not describe the free energy well enough for small droplets. This prevents the use of the analytic expressions of small droplet free energies to determine d. Hence in 3D we need to treat d as a fitting parameter.

B. Nucleation theories applied to the Ising model

The Ising model is described by the following Hamiltonian:

$$H = -J\sum_{\langle i,j\rangle} s_i s_j - h\sum_i s_i, \tag{7}$$

where $J>0$ is the coupling constant and h is the external magnetic field. The spin variable s_i at site i can be either $+1$ (up) or -1 (down), and the sum $\Sigma_{\langle i,j\rangle}$ is over nearest neighbors of the spin lattice. For convenience, we set $J=1$ in the following discussions. In our simulations, we study the relaxation of the magnetization starting from an initial state magnetized opposite to the applied field h. To be specific, we let $h>0$ and the initial state has $s_i=-1$ for most of the spins. The dynamics follows the Metropolis single-spin-flip Monte Carlo (MC) algorithm with random choice of trial spin. The simulation time step is measured in units of MC step per site (MCSS). The 2D model consists of a 100×100 square lattice and the 3D model consists of a $32\times32\times32$ simple cubic lattice, with periodic boundary conditions (PBC) applied to all directions. To avoid artifacts from finite simulation cell size, we consider (T,h) conditions such that the size of the critical droplet is much smaller than simulation cell size. We obtain nucleation rate per site and define free energy F such that $\exp(-F/k_BT)$ is proportional to the cluster population per site to present results that are invariant when the simulation cell size changes.

1. Becker-Döring theory

To compute the nucleation rate using Eq. (2) and (3), the surface free energy σ and bulk chemical potential difference $\delta\mu$ must be known for the Ising model. The chemical potential difference is simply $\delta\mu=2h$, which is a good approximation not only at low temperature but also near the critical temperature [42]. On the other hand, the surface free energy σ is more difficult to obtain. This is because the Ising model is anisotropic at the microscopic scale and the free energy of a surface depends on its orientation. Therefore, the input to the Becker-Döring theory should be an effective surface free energy σ_{eff}, which is an average over all possible orientations given the equilibrium shape of the droplet. σ_{eff} is a function of temperature T not only because the surface free energy of a given orientation depends on temperature, but also because the equilibrium shape of the droplet changes with temperature [43].

We follow the definition of Shneidman [21], which gives the analytic expression of $\sigma_{\text{eff}}(T)$ for the 2D Ising model, as shown in Fig. 1. $\sigma_{\text{eff}}(T)$ is defined in such a way that the interfacial free energy of a nucleus can be written as

$$F^{\sigma}(n) = 2\sqrt{\pi n}\,\sigma_{\text{eff}}(T) \tag{8}$$

regardless of whether its equilibrium shape determined by Wulff construction is circular or not [53]. The free energy of a droplet can be written as,

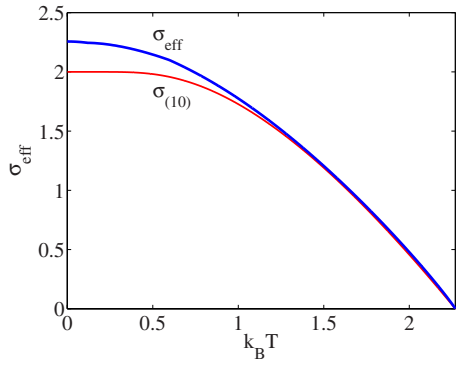

FIG. 1. (Color online) Effective surface free energy σ_{eff} as a function of temperature for the 2D Ising model from analytic expression [21]. The free energy of the surface parallel to the sides of the squares, $\sigma_{(10)}$, is also plotted for comparison.

$$F^{2D}(n) = 2\sqrt{\pi n}\sigma_{\text{eff}}(T) - 2hn \tag{9}$$

where n is the total number of up-spins in the droplet. From the maximum of $F^{2D}(n)$, we obtain the critical droplet size of the 2D Ising model,

$$n_c^{2D} = \frac{\pi\sigma_{\text{eff}}^2(T)}{4h^2} \tag{10}$$

as well as the free-energy barrier

$$F_c^{2D} = \frac{\pi\sigma_{\text{eff}}^2(T)}{2h}. \tag{11}$$

We also obtain the Zeldovich factor defined in Eq. (4)

$$\Gamma^{2D} = \sqrt{\frac{2}{k_BT}}\frac{h^{3/2}}{\pi\sigma_{\text{eff}}(T)}. \tag{12}$$

Assuming the critical droplet has a circular shape, the attachment rate can be written as

$$f_c^{+2D} = 2\beta_0(T)\sqrt{\pi n_c^{2D}} \tag{13}$$

where $\beta_0(T)$ is the average spin-flip frequency at the boundary of the droplet. As an approximation,

$$\beta_0 \approx \exp[-\sigma_{\text{eff}}(T)/k_BT]. \tag{14}$$

In the temperature and field conditions considered in this paper, the attachment rate predicted by Eqs. (13) and (14) is within a factor of 2 of the value computed by Monte Carlo simulations as shown in Appendix A. Combining all, we obtain the nucleation rate predicted by the Becker-Döring theory

$$I_{\text{BD}}^{2D}(h,T) = \beta_0(T)\sqrt{\frac{2h}{k_BT}}\exp\left[-\frac{\pi\sigma_{\text{eff}}^2(T)}{2hk_BT}\right]. \tag{15}$$

Given the analytic expressions for $\sigma_{\text{eff}}(T)$ in 2D, the predictions of the Becker-Döring theory can be computed explicitly. For example, at $k_BT=1.5$ and $h=0.05$, we have $n_c^{2D}=463$, $F_c^{2D}=46.3$, $\Gamma^{2D}=0.0034$, $f_c^{+2D}=34.0$, and $I_{\text{BD}}^{2D}=4.5\times10^{-15}$ MCSS^{-1}. The numerical results (in Sec. III B) under the same condition are $n_c=496$, $F_c=61.3$, $\Gamma=0.0033$, $f_c^{+}=39.2$, and $I=2.37\times10^{-19}$ MCSS^{-1}. As discussed further below, the four orders of magnitude discrepancy in the nucleation rate mainly comes from the underestimate of F_c^{2D} by Eq. (9). The logarithmic and constant terms in Eq. (6) are needed to remove this discrepancy.

For the 3D Ising model in a simple cubic lattice, there is no analytic expression for surface free energy for arbitrary surface orientations. A parametric expression exists only for the (100) surface [44]. Therefore, the equilibrium shape and the equivalent surface free energy of the 3D droplet are not known. Similar to Eq. (9), the free energy of a 3D droplet can be written as,

$$F^{3D}(n) = \sigma_{\text{eff}}(T)\alpha n^{2/3} - 2hn, \tag{16}$$

where $\alpha=(36\pi)^{1/3}$ is a geometric factor expressing the surface area of a sphere with unit volume. Contrary to the case of 2D Ising model, the analytic expression of $\sigma_{\text{eff}}(T)$ is not known in the 3D Ising model, and it will be used as a fitting parameter in our study.

Following the same procedures as above, we obtain the critical nucleus, free energy barrier and Zeldovich factor for the 3D Ising model,

$$n_c^{3D} = \frac{\alpha^3\sigma_{\text{eff}}^3(T)}{27h^3}, \tag{17}$$

$$F_c^{3D} = \frac{\alpha^3\sigma_{\text{eff}}^3(T)}{27h^2}, \tag{18}$$

$$\Gamma^{3D} = \sqrt{\frac{9}{\pi k_BT}}\frac{h^2}{\sqrt{\alpha^3\sigma_{\text{eff}}^3(T)}}, \tag{19}$$

$$f_c^{+3D} = \beta_0(T)\alpha n_c^{2/3}. \tag{20}$$

Finally, the nucleation rate predicted by the Becker-Döring theory is

$$I_{\text{BD}}^{3D}(h,T) = \beta_0(T)\sqrt{\frac{\alpha^3\sigma_{\text{eff}}(T)}{9\pi k_BT}}\exp\left[-\frac{\alpha^3\sigma_{\text{eff}}^3(T)}{27h^2k_BT}\right]. \tag{21}$$

Given that $\sigma_{\text{eff}}(T)$ is yet unknown and has to be treated as a fitting parameter, it is more difficult to test Eq. (21) quantitatively.

2. Langer's field theory

Langer's field theory predicts a logarithmic correction term to the droplet free energy, as in Eq. (5). In 2D Ising model, $\tau=\frac{5}{4}$, and this correction term not only increases the free energy barrier, but also increases the size of the critical droplet. The critical droplet size predicted by the field theory is,

$$n_c^{2D/FT} = \left(\frac{\sqrt{\pi}\sigma_{\text{eff}} + \sqrt{\pi\sigma_{\text{eff}}^2 + 8\pi k_BTh}}{4h}\right)^2. \tag{22}$$

This equation is to be compared with Eq. (10) predicted by the Becker-Döring theory. We will see (in Fig. 5) that Eq. (22) agrees much better with numerical results than Eq. (10),

indicating that the field theory correction should be put in the free energy function instead of the kinetic prefactor.

The $\tau k_B T \ln n$ correction term also modifies the critical nucleus size in the 3D Ising model. The analytic expression for n_c^{3D} given by the field theory can be obtained by solving a third order polynomial equation. The expression is omitted here to save space. In the 3D Ising model, there have been predictions that τ depends on temperature: $\tau=-\frac{1}{9}$ above the roughening temperature T_R [39] and $\tau=-\frac{2}{3}$ below T_R [37]. But our numerical results do not support these predictions.

III. NUMERICAL METHODS

A. Forward flux sampling

Here we give a brief overview of the FFS method used in this study. The full mathematical details can be found in the literature [32]. To compute the transition rate from the initial state A to the final state B, FFS uses a series of interfaces in the phase space defined through an order parameter λ. State A is defined as the phase space region in which $\lambda<\lambda_A$, while state B corresponds to $\lambda>\lambda_n$. The interfaces between A and B are defined as hyperplanes in the phase space where $\lambda=\lambda_i$, $i=0,1,2,\cdots,n-1$, $\lambda_A<\lambda_0<\cdots<\lambda_n$. In principle, the choice of the order parameter λ should not affect the calculated rate constant, which means λ need not be the true reaction coordinate.

In the FFS method, the nucleation rate I from A to B is expressed as a multiplication of two terms

$$I = I_0 P(\lambda_n|\lambda_0), \tag{23}$$

where I_0 is the average flux across the interface $\lambda=\lambda_0$ (i.e., leaving state A), and $P(\lambda_n|\lambda_0)$ is the probability that a trajectory leaving state A will reach state B before returning to state A again. Because it is impossible to reach interface $\lambda=\lambda_{i+1}$ without reaching interface $\lambda=\lambda_i$ first, the probability $P(\lambda_n|\lambda_0)$ can be decomposed into a series multiplication,

$$P(\lambda_n|\lambda_0) = \prod_{i=0}^{n-1} P(\lambda_{i+1}|\lambda_i), \tag{24}$$

where $P(\lambda_{i+1}|\lambda_i)$ is the probability that a trajectory reaching λ_i, having come from A, will reach λ_{i+1} before returning to A again.

In this work, we set λ to the size of the largest droplet n in the simulation cell. The rate I_0 is obtained by running a brute force Monte Carlo simulation, during which we count how frequently droplets with size larger than λ_0 are formed. An ensemble of configurations at interface $\lambda=\lambda_0$ (for trajectories coming from A) is stored from this MC simulation. We set λ_0 to be several times bigger than the average largest droplet size from the MC simulation at the given (T,h), to collect configurations that are uncorrelated with each other.

The next step is to run MC simulations with initial configurations taken from the ensemble at interface $\lambda=\lambda_0$. A fraction of the trajectories reaches interface $\lambda=\lambda_1$ before returning to state A. From these simulations the probability $P(\lambda_1|\lambda_0)$ is computed and an ensemble of configurations at interface $\lambda=\lambda_1$ is created. The process is repeated to compute the probability $P(\lambda_{i+1}|\lambda_i)$ for each $i=1,\cdots,n-1$. For each (T,h) condition, the interfaces are chosen manually such that the spacing $|\lambda_{i+1}-\lambda_i|$ between interfaces increases linearly with λ_i, with the first spacing $|\lambda_1-\lambda_0|$ large enough to have $P(\lambda_1|\lambda_0)\leq 10^{-1}$. The nucleation rate constant turns out to be the same within statistical error when computed with different sets of interfaces having larger spacings than above. The last interface λ_n is chosen to be 3 to 4 times bigger than the critical nucleus size to ensure that the stable state is reached.

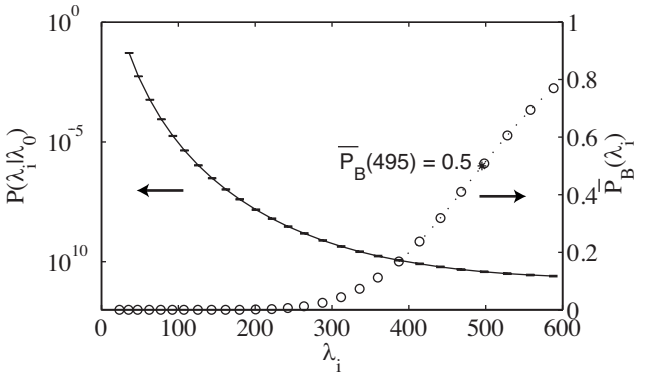

FIG. 2. The probability $P(\lambda_i|\lambda_0)$ (solid line) of reaching interface λ_i from λ_0 and average committor probability $\overline{P_B}(\lambda_i)$ (circles) over interface λ_i at $(k_BT,h)=(1.5,0.05)$ for the 2D Ising model. The 50% committor point is marked by *.

As an example, Fig. 2 plots the probability $P(\lambda_i|\lambda_0) \equiv P(\lambda_1|\lambda_0)P(\lambda_2|\lambda_1)\cdots P(\lambda_i|\lambda_{i-1})$ for the 2D Ising model at $k_BT=1.5$ and $h=0.05$. In this test case, we find $I_0=1.45\times10^{-8}$ MCSS^{-1} with $\lambda_0=24$ from a brute force Monte Carlo simulation with 10^7 MCSS. 15 000 configurations are then collected at each interface, which allows the nucleation rate to be determined within 5%. The probability of reaching interface $\lambda=\lambda_n$ from interface $\lambda=\lambda_0$ is $P(\lambda_n|\lambda_0)=1.92\times10^{-11}$ with $\lambda_n=1200$. Following Eq. (23), the nucleation rate under this condition is $I^{\mathrm{FFS}}=2.78\times10^{-19}$ MCSS^{-1}.

It is important to note that FFS does not require the transitions between different interfaces to be Markovian. Neither does it require the transitions to satisfy detailed balance, unlike other sampling methods [19,45,47]. Therefore, it can be used to test the fundamental assumption of the Becker-Döring theory, which states that the nucleation process can be coarse-grained into a one-dimensional Markov chain. FFS would fail if there is no separation of time scale, i.e., if the time spent on a reaction path is comparable to (instead of much shorter than) the dwell time in state A or state B. In order to test the applicability of FFS to Ising models, we benchmark it against brute-force MC simulations of the 3D Ising model at $k_BT=0.59T_c$ and $h=0.589$. The nucleation rate computed by FFS, $I^{FFS}=4.10\times10^{-10}$ MCSS^{-1}, is in good agreement with the brute-force MC result [29,30], $I^{MC}=5.81\times10^{-10}$ MCSS^{-1}, confirming the applicability of FFS.

B. Computing rate from Becker-Döring theory

Having computed the nucleation rate from FFS, we will use it as a benchmark and compare it with the nucleation rate

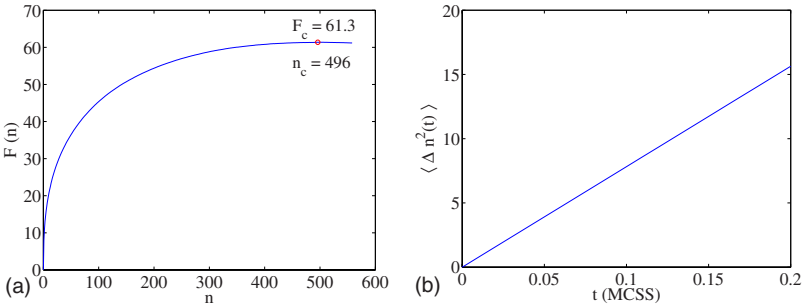

FIG. 3. (Color online) (a) Droplet free energy $F(n)$ obtained by U.S. at $k_BT=1.5$ and $h=0.05$ in the 2D Ising model. (b) Fluctuation of droplet size $\langle \Delta n^2(t) \rangle$ as a function of time.

predicted by the Becker-Döring theory. To gain more insight from this comparison, we will split the Becker-Döring theory into two parts and test them separately. Part I is summarized in Eq. (3), which expresses the nucleation rate in terms of the attachment rate f_c^+, Zeldovich factor Γ, and the free energy barrier F_c. Part II is the prediction of the droplet free energy $F(n)$, which was discussed in Sec. II B.

We will compute the droplet free energy $F(n)$ numerically by umbrella sampling (U.S.) [18]. The result then allows us to specifically test Part II of the Becker-Döring theory. To test Part I of the Becker-Döring theory, we will compute F_c and Γ from the free energy function $F(n)$ obtained by U.S., and plug them into Eq. (3). The attachment rate f_c^+ can also be computed separately, as explained below.

As an example, Fig. 3(a) shows the droplet free energy $F(n)$ computed from U.S. at $k_BT=1.5$ and $h=0.05$. The order parameter is the size of the largest droplet, n. A parabolic bias function $0.1k_BT(n-\bar{n})^2$ is used, where $\bar{n}$ is the center of each sampling window, following Auer and Frenkel [18]. The maximum of this curve indicates that the critical droplet size is $n_c=496$ and the free-energy barrier is $F_c=61.3$. The Zeldovich factor can be calculated from the second derivative of this curve at n_c, which gives $\Gamma=0.0033$.

We then collect many configurations from the U.S. simulation, when the bias potential is centered at the critical droplet size. Using each configuration as an initial condition, we run Monte Carlo simulations and obtain the effective attachment rate from the following equation,

$$f_c^+ = \frac{\langle \Delta n^2(t) \rangle}{2t}, \tag{25}$$

where $\langle \Delta n^2(t) \rangle$ is the mean square fluctuation of the droplet size. $\Delta n(t) \equiv n(t) - n(t=0)$, $n(t)$ is the droplet size at time t, and $\langle\ \rangle$ represents ensemble average from these Monte Carlo simulations. The Monte Carlo simulations are stopped when $|\Delta n(t)|$ exceeds 4. The result for the means square fluctuation $\langle \Delta n^2(t) \rangle$ at $k_BT=1.5$ and $h=0.05$ is plotted in Fig. 3(b), which shows a linear function of time. From the slope of this curve, we obtain $f_c^+=39.1$ MCSS^{-1}. A similar approach was used by Brendel *et al.* [24] to compute the interface diffusion coefficient.

Combining the values of f_c^+, Γ, F_c and plug them into Eq. (3), we find that the Becker-Döring theory would predict the nucleation rate to be $I^{\mathrm{BD}}=2.37\times10^{-19}$ MCSS^{-1}, if the correct free energy function $F(n)$ is used. This is very close to the FFS result $I^{\mathrm{FFS}}=2.78\times10^{-19}$ MCSS^{-1} given in the previous section. The agreement confirms the validity of Part I of the Becker-Döring theory. Comparisons over a wider range of conditions are presented in the following section.

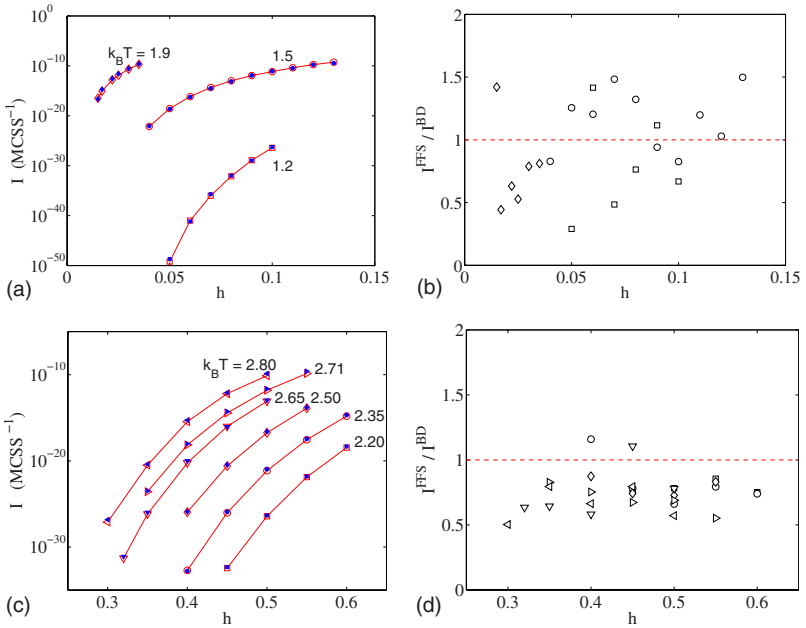

FIG. 4. (Color online) The nucleation rate I computed by FFS (open symbols) and Becker-Döring theory with U.S. free energies (filled symbols) in the (a) 2D and (c) 3D Ising models. The ratio between nucleation rates obtained by FFS and Becker-Döring theory at different temperatures in the (b) 2D and (d) 3D Ising models. The symbols in (b) and (d) match those defined in (a) and (c), respectively.

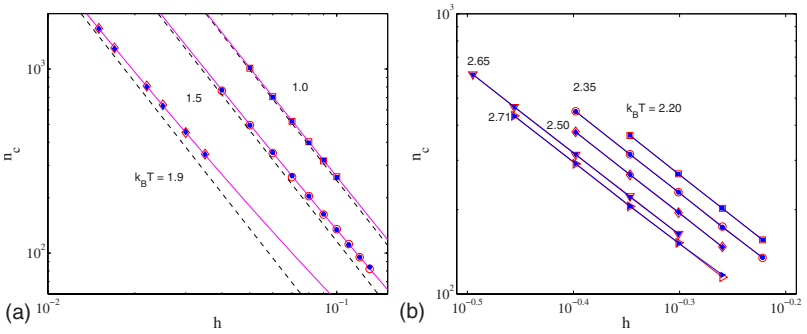

FIG. 5. (Color online) (a) For 2D Ising model, the critical droplet size n obtained from FFS (filled symbols) and umbrella sampling (open symbols). n_c predicted by Becker-Döring theory (dotted line) and by field theoretic equation (solid line) are plotted for comparison. (b) For 3D Ising model, the critical droplet size n obtained from FFS (filled symbols) and umbrella sampling (open symbols).

IV. RESULT

A. Nucleation rate

We have computed the nucleation rates using two different methods over a wide range of conditions: $h=0.01-0.13$, $T=0.5-0.8T_c$ for 2D and $h=0.30-0.60$, $T=0.4-0.7T_c$ for 3D, where T_c is the critical temperature at zero field ($k_BT_c=2.269$ in 2D and 4.512 in 3D). In the first method, the nucleation rate is directly computed by FFS. In the second method, the nucleation rate is computed from the Becker-Döring Eq. (3), but using the free energy curve obtained from U.S., as described in Sec. III B. The pre-exponential factor, $f_c^+\Gamma$, is found to have a weak dependence on T and h (see Appendix A), and varies by about a factor of 2 in the entire range of T and h considered in this study. The calculations are performed on a 3 GHz Linux cluster. Each FFS calculation for a given (T,h) condition takes about 50 CPU-hours for the 2D Ising model and 200 CPU-hours for the 3D Ising model. Each U.S. calculation takes a similar amount of time as an FFS calculation.

As shown in Fig. 4, the nucleation rate over these conditions spans more than 20 orders of magnitude. Yet, most of the rates predicted by the two methods are within 50% of each other. This is a strong confirmation of Part I of the Becker-Döring theory, i.e., Equation (3). It confirms that for the purpose of computing nucleation rate, it is valid to coarse grain the Ising model to a one-dimensional Markov chain, with the size of the largest droplet being the reaction coordinate. Detailed balance between neighboring states along the Markov chain, as is assumed by the Becker-Döring theory, has been shown by a recent study [27] and our confirmation of Eq. (3) provides another evidence for it. This means that the Becker-Döring theory can predict the nucleation rate of the 2D and 3D Ising models accurately, provided that the correct free energy function $F(n)$ is used. This is consistent with an earlier report by Brendel *et al.* [24].

B. Critical droplet size

There are two common definitions of the critical droplets. In the first definition, a droplet is of critical size if its probability to grow and cover the entire system is 50%. In other words, a critical droplet has a committor probability of 50%. In the second definition, a droplet is of critical size if it corresponds to the maximum of the free energy curve $F(n)$. It is of interest to verify whether these two definitions are equivalent.

After each FFS simulation under a given (T,h) condition, an ensemble of 15,000 spin configurations are saved at each interface λ_i. The average values of $\overline{P_B(\lambda_i)}$ for a given interface can be estimated using the following recursive relation,

$$\overline{P_B(\lambda_i)} = \overline{P_B(\lambda_{i+1})}P(\lambda_{i+1}|\lambda_i) \tag{26}$$

for $i=n-1,n-2,\ldots 1$ with the boundary condition $\overline{P_B(\lambda_n)}=1$ [46]. By fitting the data of $\overline{P_B}$ to a smooth curve with spline interpolation, we can extract the critical value n_c for which $\overline{P_B}=0.5$, as shown in Fig. 2. Some of the critical nucleus size obtained this way are shown in Fig. 5 as filled symbols.

The droplet sizes that correspond to the maximum of the free energy curve obtained by U.S. are listed in Fig. 5as open symbols. For both 2D and 3D Ising models, critical size from two different methods agree with each other within 2%. This confirms that the two definitions for the critical nucleus are equivalent, provided that the correct free energy curves $F(n)$ are used. It also proves that the size of the largest droplet is a good reaction coordinate.

Figure 6(a) plots the histogram of the committor probability for an ensemble of spin configurations with $n=496$ for the 2D Ising model at $k_BT=1.5$ and $h=0.05$. The average committor probability of this ensemble is 49.4%. About 94% of the spin configurations in this ensemble have committor probabilities within the range of $49\pm5\%$. This further con-

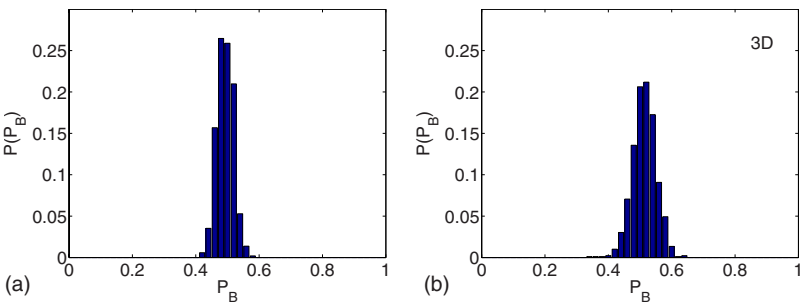

FIG. 6. (Color online) (a) Histogram of committor probability in an ensemble of spin configurations with $n=496$ for the 2D Ising model at $k_BT=1.5$ and $h=0.05$. Representative droplets are also shown, with black and white squares corresponding to +1 and −1 spins, respectively. (b) Histogram of committor probability in an ensemble of spin configurations with $n=524$ for the 3D Ising model at $k_BT=2.20$ and $h=0.40$.

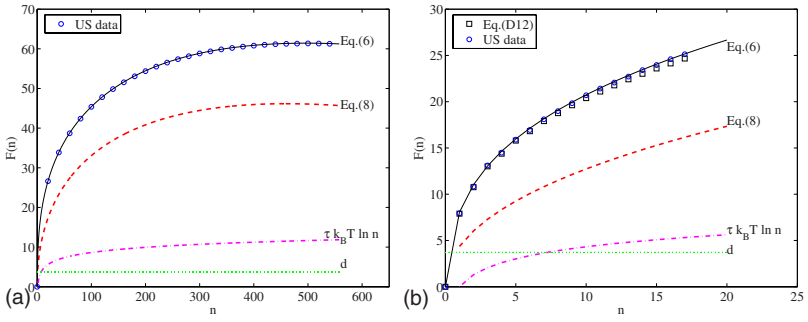

FIG. 7. (Color online) (a) Droplet free energy curve $F(n)$ of the 2D Ising model at $k_BT=1.5$ and $h=0.05$ obtained by U.S. (circles) is compared with Eq. (6) (solid line) and Eq. (9) (dashed line). Logarithmic correction term $\frac{5}{4}k_BT\ln n$ (dot-dashed line) and the constant term d (dotted line) are also drawn for comparison. (b) Magnified view of (a) near $n=0$, together with the results from analytic expressions (squares) available for $n\leq 17$ (see Appendix D).

firms that the size of the largest cluster, n, is a very good reaction coordinate of the nucleation process. Figure 6(b) plots the histogram of the committor probability within an ensemble of spin configurations with $n=524$ for the 3D Ising model at $k_BT=2.20$ and $h=0.40$. The average committor probability of this ensemble is 50%. About 80% of the spin configurations in this ensemble have committor probabilities within the range of $50\pm5\%$. The spread of the committor probability distribution is wider than the 2D case, and is consistent with an earlier report [25].

C. Droplet free energy of 2D Ising model

The previous sections show that the Becker-Döring theory performs well as long as the correct droplet free energy $F(n)$ is provided. We now compare the theoretical predictions of $F(n)$ with numerical results by U.S. We will focus on 2D Ising model in this section and will discuss $F(n)$ in the 3D Ising model in the next section.

Figure 7 plots the $F(n)$ curves for $k_BT=1.5$ and $h=0.05$. Numerical results from U.S. and predictions from the Becker-Döring theory, Eq. (9), and Langer's field theory, Eq. (6), are plotted together. It is clear that the logarithmic correction term $\tau k_BT\ln n$ from the field theory is substantial. The field theory prediction, which contains this correction term, agrees very well with numerical U.S. results (after the constant term is added, see Appendix D). The free energy used in CNT, Eq. (9), which lacks this correction term, is significantly lower. Obviously, if this free energy curve is used, the Becker-Döring theory will overestimate the nucleation rate by several orders of magnitude. Our result also shows that, the field theory predictions, though derived under the assumption of infinitesimal h, are still valid at finite h in the range of field considered in this study.

Our results shows that the macroscopic surface free energy (at zero h) can be safely applied to a droplet (at finite h) [29], provided that the constant correction term is added (see Appendix D). Brendel *et al.* [24] reported that the effective surface free energy exceeds that of the macroscopic surface free energy by 20%. But this was caused by the neglect of the logarithmic correction term in that study.

Our results contradict the previous report [21] that τ is close to zero at low temperatures ($T=0.59T_c$ and $0.71T_c$) and only goes to $\frac{5}{4}$ near $T=0.84T_c$. In the previous study [21], only small clusters ($n<60$) are sampled, but not using the umbrella sampling technique. We suspect this approach is susceptible to the error caused by the lack of statistics at low temperatures (especially for clusters with $n>30$). Because the field theoretic correction term $\tau k_BT\ln n$ becomes smaller at low T, it could be masked by the statistical error. To support our finding, the free energy curves for cluster sizes up to $n=1950$ at a wide temperature range (from $0.53T_c$ to $0.84T_c$) are attached in a supplementary document [48]. $\tau=\frac{5}{4}$ is necessary in the entire temperature range to accurately describe the droplet free energy.

In the literature, the field theory correction is usually expressed as an extra pre-exponential factor inserted into the Becker-Döring formula of the nucleation rate. Both a pre-exponential factor and a change to the free-energy curve can modify the nucleation rate. So it may appear impossible (or irrelevant) to decide which approach is more "correct." However, a closer inspection shows that it is indeed possible to tell whether the correction should be interpreted as a free energy change, or a kinetic prefactor. This is because self-consistency requires that the maximum of the free-energy curve $F(n)$ should match the droplet size n_c whose committor probability is 50%, as discussed in Sec. IV B.

Figure 5 shows the critical droplet sizes $n_c^{F/\mathrm{BD}}$ (dotted lines), which correspond to the maximum of the free energy curves $F(n)$ predicted by the Becker-Döring theory, Eq. (9). They are significantly smaller than the critical droplet sizes n_c^{comm} (filled symbols) that corresponds to a 50% committor probability. With the field theory correction term in the free energy, the critical droplet sizes $n_c^{F/\mathrm{FT}}$ (solid lines) agree much better with n_c^{comm}. This result clearly shows that the field theory correction should be placed in the free energy function $F(n)$, instead of being a kinetic prefactor.

It is of interest to compare the various free energy expressions discussed so far with the analytic (exact) expressions [49] for $F(n)$ that are available for $0\leq n\leq 17$. It is somewhat surprising that the field theory prediction of $F(n)$ (after corrected by a constant term, see Appendix D) agrees very well with both the numerical data from U.S. and the analytic expressions, for such small values of n. This is another confirmation for the field theory prediction of the free-energy curve, Eq. (6).

Shneidman *et al.* [21] also observed the effect of the logarithmic correction term, but expressed it in terms of "size-dependent prefactor," and suspected that it is caused by coagulation of droplets. Our results show that this is not a coagulation (many-droplet) effect, because the logarithmic correction term is derived by considering the shape fluctuation of a single droplet.

In summary, the free-energy expression from CNT must be modified by two terms, i.e., a logarithmic correction term $\tau k_BT\ln n$ from field theory and a constant term to match the

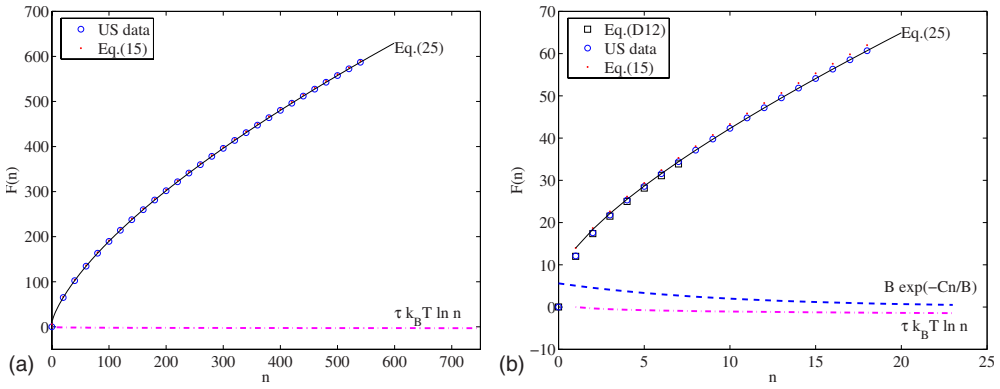

FIG. 8. (Color online) (a) Droplet free energy $F(n)$ of the 3D Ising model at $k_BT=2.40$ and $h=0$ obtained by U.S. (circles) is compared with Eq. (30) (solid line) and Eq. (16) (dots). Logarithmic term $\tau k_BT \ln n$ is also plotted (dot-dashed line). The difference in predictions by classical expression Eq. (16) and field theory Eq. (30) are very small compared to $F(n)$ itself and cannot be observed at this scale. (b) Magnified view of (a) near $n=0$, together with the analytic solution of small droplets (squares, see Appendix D) and the exponential correction term (dashed line).

free energy of very small droplets. In 2D, both terms can be determined completely from existing theories and contain no fitting parameters.

D. Droplet free energy of 3D Ising model

In the following, we will examine the functional form of the droplet free energy $F(n)$ in the 3D Ising model. Because there is no analytic solution to the effective surface free energy in 3D, $\sigma_{\text{eff}}(T)$ must be treated as a fitting parameter in our analysis, which creates more uncertainty in our conclusions. For example, we cannot unambiguously determine the coefficient τ in the logarithmic correction term [in Eq. (6)] from the numerical results. Another difficulty in determining τ is that in 3D the logarithmic correction term is much smaller compared with the first two terms in Eq. (6).

To reduce the complexity from finite h, we computed droplet free energy at zero field for a range of temperature $k_BT=2.0,\ldots,2.8$ by U.S. Figure 8 plots the results at $k_BT=2.40$ and $h=0$. We have examined a number of functional forms to see which one best describes the numerical data of the droplet free energy.

First, we fit the data to the original Becker-Döring form, Eq. (16), plus a constant correction term, i.e.,

$$F(n) = \sigma_{\text{eff}}(T)\alpha n^{2/3} - 2hn + d(T), \tag{27}$$

where $\sigma_{\text{eff}}(T)$ is a free fitting parameter at each temperature. We find that Eq. (27) cannot describe the droplet free energy well in the entire range of n. Since we expect it to be more accurate in the continuum limit of large n, we fit the U.S. data to Eq. (27) only in the range of $n>50$. The resulting term $d(T)$ is in the range of -1.1 (at $k_BT=2.0$) to -2.4 (at $k_BT=2.8$). The error in the fit is defined as $R \equiv [\frac{1}{700}\Sigma_{i=50}^{750}(F(i)-F_{\text{fit}}(i))^2]^{1/2}$, where $F(i)$ is the numerical data from U.S., and $F_{\text{fit}}(i)$ is the value given by Eq. (27). The resulting R is in the range of 0.01–0.13 and increases with increasing temperature. Significant discrepancy between the U.S. data and the fit is observed in the range of $n<50$, which will be further discussed below.

The next function to be considered for the fit includes the logarithmic correction term,

$$F(n) = \sigma_{\text{eff}}(T)\alpha n^{2/3} + \tau(T)k_BT \ln n - 2hn + d(T) \tag{28}$$

in which τ is a free parameter for each temperature T. The error of the fit is now reduced to about $R\approx 0.01$ for all temperatures and is now independent of temperature. This means that the logarithmic term improves the description of the temperature dependence of the free energy of large droplets ($n>50$). But the discrepancy in the range of $n<50$ still remains. This is different from the 2D Ising model, where Eq. (6) describes the droplet free energy very well even without any fitting parameters.

Perini *et al.* [39] used the following functional form to fit their free-energy data,

$$F(n) = \sigma_{\text{eff}}(T)\alpha n^{2/3} + K(T)n^{1/3} + \tau k_BT \ln n - 2hn + d(T) \tag{29}$$

where $\tau=-\frac{1}{9}$ is constrained to be a constant [54]. The parameter K corresponds to the extra energy of "ledges" that appear on 3D droplets. We find that the quality of the fit using Eq. (29) is similar to that using Eq. (28) [55]. However, the resulting $K(T)$ is an increasing function of temperature. This is counter-intuitive because the continuum droplet approximation is expected to be better at higher temperatures where equilibrium droplet shape become more spherical. Hence, we would expect $K(T)$ to decrease with increasing temperature. Therefore, we believe Eq. (28) is a more appropriate functional form than Eq. (29).

Hence, we do not include the "ledge" energy term, and will treat τ as a function of temperature during the fitting. We also find that the fit in the range of $n<50$ can be significantly improved by adding an exponential term. The data at all T and in the entire range of $0<n<750$ considered in this study turns out to be well fitted by the following function.

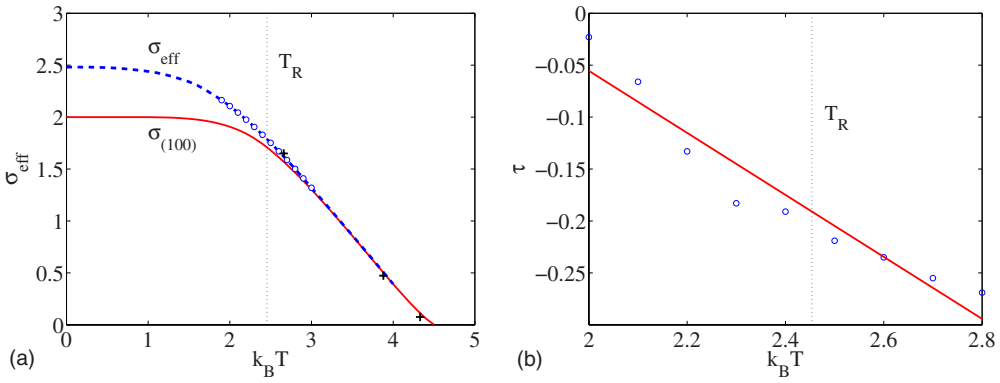

FIG. 9. (Color online) (a) Surface free energies of the 3D Ising model as functions of temperature. Circles are fitted values of σ_{eff} from Eq. (30), dashed line is the expected behavior of σ_{eff} over a wider range of temperature, and solid line is the free energy of the (100) surface [44]. Numerically fitted values of σ_{eff} from Heermann *et al.* [29] are plotted as +. (b) τ values that give the best fit to the free energy data from U.S. τ can be roughly described by a linear function of T shown as a straight line. No abrupt change is observed near the roughening temperature T_R.

$$F(n) = \sigma_{\text{eff}}(T)\alpha n^{2/3} + \tau(T)k_BT \ln n - 2hn + A + B(T)\exp\left[-\frac{Cn}{B(T)}\right], \tag{30}$$

where A and C are constants independent of T, and $B(T)$, $\sigma_{\text{eff}}(T)$, and $\tau(T)$ are functions of T [56]. The fitted parameters are: $A=0.06$ and $C=0.59$. It turns out that $B(T)$ can be well described by a linear function: $B(T)=9.12k_BT-16.08$. The contribution of the exponential term is plotted in Fig. 8(b). In the range of T and h considered in this study, the size of the critical nucleus is larger than 100. Hence the nucleation rate predicted by CNT under these conditions is only affected by $F(n)$ in the range of $n>100$. When Eq. (30) is used, the numerical values of the logarithmic term is in the range of -5 to 0, for $2.0\leq k_BT\leq 2.8$ and $100<n<750$. It is the major correction term to the classical expression of the droplet free energy, Eq. (16), for $n>100$. In comparison, the constant term is $A=0.06$ and the magnitude of the exponential term is less than 10^{-7} for $n>100$.

Figure 9(a) shows the fitted values of σ_{eff} in the temperature range of $0.4-0.65T_c$. σ_{eff} decreases with T, as expected. In the limit of large T, the difference between the free energies of (100) and (110) surfaces diminishes, the droplet becomes spherical, and σ_{eff} converges to the free energy of (100) surfaces. In the limit of $T\to 0$, we expect σ_{eff} to converge to $(6/\pi)^{1/3}$ times the surface tension of the (100) surface. This is because as $T\to 0$, the shape of the droplet becomes cubical [28], and $(6/\pi)^{1/3}$ is the surface area ratio between a sphere and a cube, both having unit volume. The expected shape of $\sigma_{\text{eff}}(T)$ over this temperature range is plotted as a dashed line, which is similar to the case of 2D Ising model shown in Fig. 1. In summary, we expect σ_{eff} to decrease from 2.481 to 0 as temperature increases. For example, at $k_BT=2.71$, $\sigma_{\text{eff}}=1.6$. This may explain the discrepancy reported by Pan *et al.* [25], in which $\sigma_{\text{eff}}=2$ is assumed at $k_BT=2.71$. In Vehkamaki *et al.* [30], the nucleation rate predicted by CNT was reported to have a weaker temperature dependence than the numerical results. This is probably caused by the use of the same surface free energy (at $T=0.59T_c$) in the entire temperature range ($0.54T_c$ to $0.70T_c$). The decrease of surface energy with temperature leads to a significant reduction of nucleation free energy barrier with temperature. This corresponds to an anomalously large "effective entropy" of nucleation (see Appendix B), which would be difficult to explain if the variation of surface energy were ignored.

Figure 9(b) shows the fitted values of τ as a function of temperature. Over the range of temperature considered here, τ can be approximated by a linear function of T, $\tau=-0.26k_BT+0.44$. The fact that $\tau<0$ in 3D is consistent with theoretical predictions. But τ is found to decrease with temperature, and no discontinuity at the roughening temperature is observed. This is consistent with the observation that no significant change of droplet shape occurs near the roughening temperature (see Appendix C). This is contrary to the theoretical predictions of $\tau=-\frac{2}{3}$ at $T<T_R$ and $\tau=-\frac{1}{9}$ at $T>T_R$. The change of τ with T may be the consequence of a gradual change of anisotropy effects as temperature changes [40]. More investigation is needed to resolve the controversy of τ in the 3D Ising model. The difference between 2D (where $\tau=5/4$ remains a constant) and 3D Ising models on the behavior of τ remains intriguing.

V. SUMMARY

In this paper, we have used two independent methods to calculate the nucleation rate of Ising model in 2D and 3D, in order to check independently the different assumptions of the nucleation theories. The Markov chain assumption with the largest droplet size as the reaction coordinate is found to be accurate enough to predict nucleation rate spanning more than 20 orders of magnitude, provided that the correct droplet free energy function is used. The logarithmic correction term is found to be essential to droplet free energy in 2D. Our numerical results verified the field theory prediction that $\tau=5/4$ in 2D. However, for the 3D Ising model, our numerical results are not consistent with existing theories on the coefficient τ of the logarithmic correction term, suggesting that some important physics may still be missing in the ex-

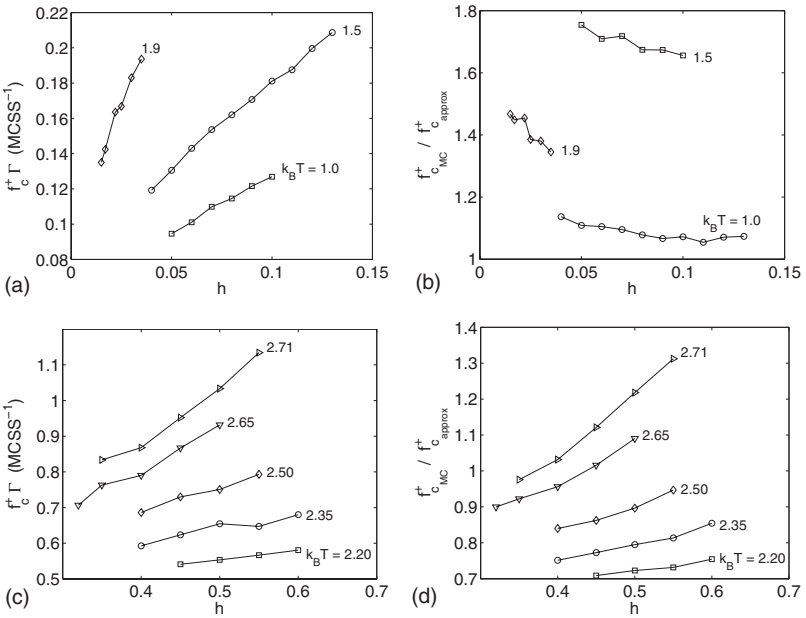

FIG. 10. (a) The pre-exponential factor $f_c^+\Gamma$ in 2D computed from Monte Carlo and U.S. (b) The ratio between the attachment rate f_c^+ in 2D computed by Monte Carlo and that predicted by Eq. (13). (a) The pre-exponential factor $f_c^+\Gamma$ in 3D computed from Monte Carlo and U.S. (b) The ratio between the attachment rate f_c^+ in 3D computed by Monte Carlo and that predicted by Eq. (20).

isting theories, such as the anistropy effect on the droplet free energy. An exponential function seems to be necessary to describe the free energy of small 3D droplets, but it is not needed for the 2D droplets. A promising direction for future research is to numerically compute the surface free energy of different orientations in 3D and to build the effective surface free energy σ_{eff} from the Wulff construction. This would eliminate σ_{eff} as a fitting parameter and would enable a more stringent test of CNT for the 3D Ising model. In addition, 3D simulations at smaller h values will allow a more direct comparison with existing nucleation theories, most of which assume an infinitesimal h.

APPENDIX A: ATTACHMENT RATE

In this appendix, we examine the dependence of the pre-exponential factor, $f_c^+\Gamma$, in the nucleation rate predicted by the Becker-Döring theory, Eq. (3), on T and h. In the (T,h) conditions considered in this study, both the attachment rate f_c^+ and the Zeldovich factor Γ vary by several orders of magnitude. However, their variations largely cancel each other and the product $f_c^+\Gamma$ only varies within a factor of 2, as shown in Figs. 10(a) and 10(c).

Equation (4) defines the Zeldovich factor Γ in terms of the second derivative of the droplet free energy function $F(n)$ which is discussed in more detail in the following appendices. Here we focus on the attachment rate f_c^+ and evaluate the quality of the approximations in Eqs. (13), (14), and (20). Figures 10(b) and 10(d) plots the ratio of the attachment rate f_c^+ computed from Monte Carlo and that predicted by the classical theories, in 2D and 3D respectively. The predictions from classical theories are within a factor of 2 of the numerical results for the entire (T,h) conditions considered in this work. The discrepancy between theoretical and numerical results observed here can be partly attributed to the approximation that the droplet is circular in 2D, as in Eq. (13) or spherical in 3D, as in Eq. (20). Due to the discreteness of the Ising model, this is obviously not the case, as shown in Appendix C.

APPENDIX B: EFFECTIVE ENTROPY OF NUCLEATION

The purpose of this appendix is to examine the temperature dependence of droplet free energy at a given h, for both 2D and 3D Ising models. Figure 11(a) plots the droplet free energy as a function of droplet size n for the 2D Ising model at $h=0.1$ and different temperatures. The maxima of these curves, i.e., the free-energy barrier F_c, are plotted in Fig. 11(b). The data can be fitted to a straight line, whose slope gives an effective entropy of $S=43.5k_B$. An entropy of this magnitude seems anomalously large and will be difficult to attribute to the shape fluctuation of the critical droplet. We believe that this entropy is a consequence of the temperature dependence of the effective surface free energy $\sigma_{\text{eff}}(T)$. In CNT, the free-energy barrier is linked to $\sigma_{\text{eff}}(T)$ through Eq. (11). As a comparison, Fig. 11(b) also plots the prediction of Eq. (11) as a dashed line, which gives an effective entropy of $53.4k_B$. This confirms that the anomalously large entropy is a result of the temperature dependent surface tension. The large difference between the solid line and dashed line indicates the importance of the logarithmic correction term in 2D.

Figure 11(c) plots the droplet free energy as a function of droplet size n for the 3D Ising model at $h=0.45$ and different temperatures. The maxima of these curves, i.e., the free energy barrier F_c, are plotted in Fig. 11(d). The data can be fitted to a straight line, whose slope gives an effective entropy of $S=143k_B$. As a comparison, Fig. 11(b) also plots the prediction of CNT, Eq. (18), as a dashed line, which gives an effective entropy of $152k_B$. Again, the anomalously large entropy is a result of the temperature dependent surface tension.

APPENDIX C: DROPLET SHAPES

The purpose of this appendix is to examine the shape change of the droplets as temperature changes. As

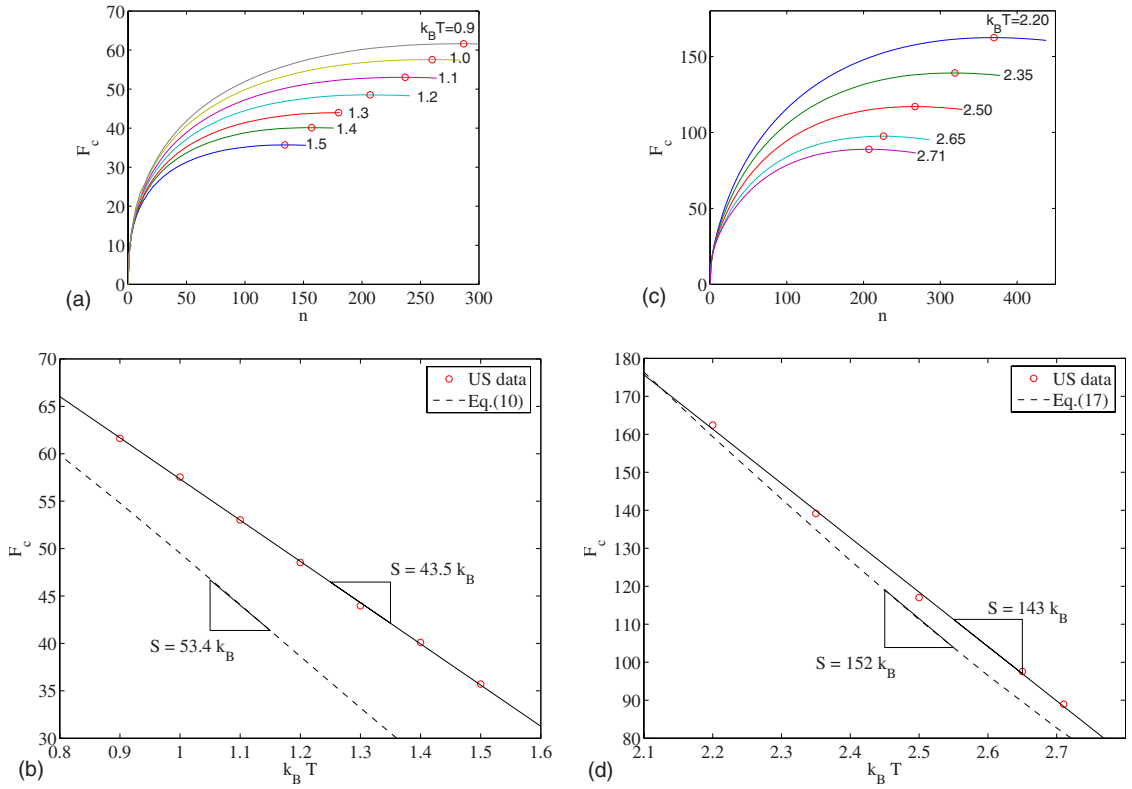

FIG. 11. (Color online) (a) Droplet free energy as a function of droplet size n at $h=0.1$ and different k_BT for the 2D Ising model. The critical droplet free energy is marked by circles. (b) Critical droplet free energy (circles) from (a) as a function of k_BT for the 2D Ising model. The solid line is a linear fit of the data, and the dashed line is the prediction of Eq. (11). (c) Droplet free energy as a function of droplet size n at $h=0.45$ and different k_BT for the 3D Ising model. (d) Critical droplet free energy from (c) as a function of k_BT for the 3D Ising model. The solid line is a linear fit of the data, and the dashed line is the prediction of Eq. (18).

temperature increases, we reduce the magnitude of the field h, so that the size of the critical nucleus stays roughly the same. The droplets plotted here are close to the critical size and are randomly chosen from FFS simulations.

Figure 12(a) shows three droplets in 2D at $k_BT=1.0$, 1.5 and 1.9. At $k_BT=1.0$, the droplet has long facets on the boundary and a solid interior. At $k_BT=1.5$, the droplet shape becomes more circular than rectangular. At $k_BT=1.9$, significant fluctuation can be observed on the droplet surface. The inside of the droplet also becomes more porous containing a number of -1 spins.

Figure 12(b) shows three droplets in 3D at $k_BT=2.2$, 2.5 and 2.71. At $k_BT=2.0$ (below the roughening temperature), small facets can be found on the droplet surface. At $k_BT=2.5$ (near the roughening temperature), the droplet shape does not seem to be substantially different from that at $k_BT=2.0$. At $k_BT=2.71$ (above the roughening temperature), the surface shape becomes more irregular. The droplet shape seems to change gradually with increasing temperature, without any sharp transition (resembling a phase transition) at the roughening temperature T_R. This may be caused by the small size the critical droplet in this study, which prevents a true roughening transition of its surface morphology due to its small area.

APPENDIX D: THE CONSTANT TERM IN DROPLET FREE ENERGY

In this appendix, we discuss how to obtain the constant correction term in the droplet free energy function, Eq. (6), for the 2D Ising model by considering the exact free energy expressions of small clusters. Shneidman *et al.* [21] used a similar approach to improve the predictions of droplet distributions. A related problem was discussed by Wilemski [50]. We will also list the free energy expressions of small 3D clusters. Even though they cannot be used to determine the constant correction term, they are useful for comparison purposes, as in Fig. 8(b).

Because the free-energy expression, Eq. (5), is based on a continuum droplet model, we expect it to be inaccurate for very small droplets, where the discreteness of the lattice becomes appreciable. On the other hand, the continuum approximation should work better for large clusters, i.e., in the continuum limit. Therefore, we expect that Eq. (5) can be used to accurately predict the free energy difference between two large droplets, $F(m)-F(n)$, if both $m \gg 1$ and $n \gg 1$. This justifies the addition of a constant term in Eq. (6). The value of the constant term can be determined by matching Eq. (6) with the exact values of $F(n)$ for small n.

Fortunately, for small enough n, the exact expression of the droplet free energy can be written down by enumerating

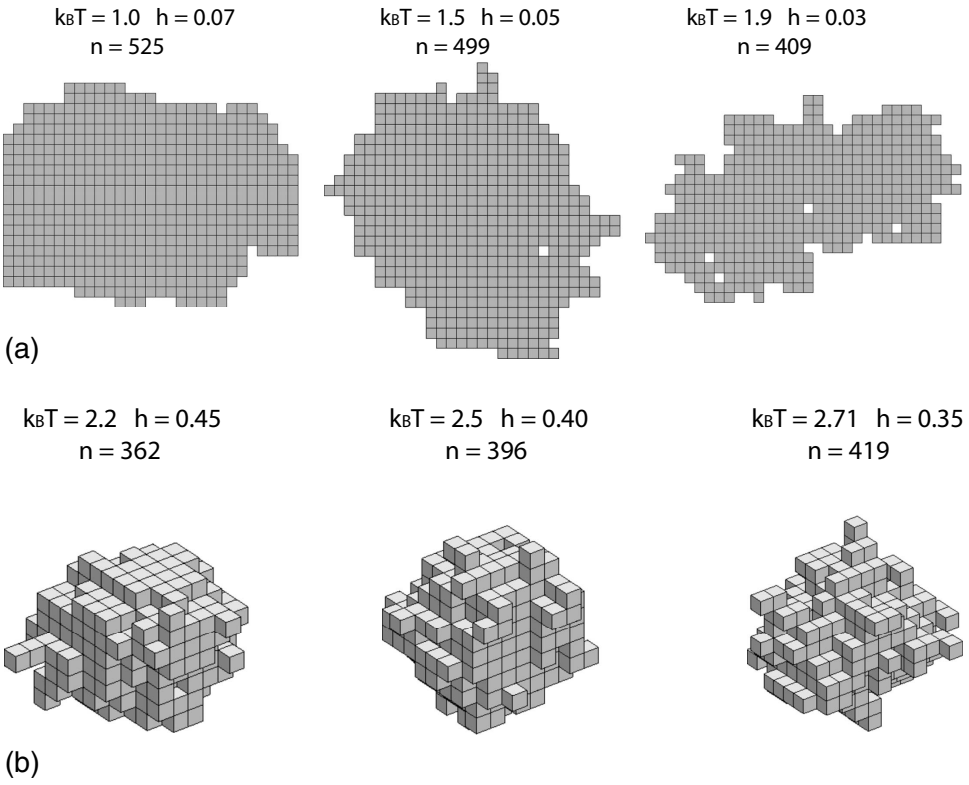

FIG. 12. Droplets in (a) 2D and (b) 3D Ising models randomly chosen from FFS simulations at different (T,h) conditions. n is the size of the droplet.

all possible shapes of the droplet with size n and summing up their contributions to the partition function. For simplicity, we will consider the case of $h=0$. For example, a droplet of $n=1$ is simply an isolated spin +1 surrounded by spins −1. The partition function of this droplet in the 2D Ising model is,

$$\Omega_1^{2D} = e^{-8\beta J}, \tag{D1}$$

where $\beta \equiv 1/(k_B T)$. Similarly, the partition function of droplets of size 2, 3, and 4 are,

$$\Omega_2^{2D} = 2e^{-12\beta J}, \tag{D2}$$

$$\Omega_3^{2D} = 6e^{-16\beta J}, \tag{D3}$$

$$\Omega_4^{2D} = e^{-16\beta J} + 18e^{-20\beta J}. \tag{D4}$$

The number in front of the exponential term corresponds to the multiplicity of clusters of a given shape. Analytic expressions for the partition functions of 2D droplets have been obtained up to $n=17$ with computer assistance [49].

We have obtained similar expressions for the droplet partition functions in the 3D Ising model for n from 1 to 7.

$$\Omega_1^{3D} = e^{-12\beta J}, \tag{D5}$$

$$\Omega_2^{3D} = 3e^{-20\beta J}, \tag{D6}$$

$$\Omega_3^{3D} = 15e^{-28\beta J}, \tag{D7}$$

$$\Omega_4^{3D} = 3e^{-32\beta J} + 83e^{-36\beta J}, \tag{D8}$$

$$\Omega_5^{3D} = 48e^{-40\beta J} + 486e^{-44\beta J}, \tag{D9}$$

$$\Omega_6^{3D} = 18e^{-44\beta J} + 496e^{-48\beta J} + 2967e^{-52\beta J}, \tag{D10}$$

$$\Omega_7^{3D} = 8e^{-48\beta J} + 378e^{-52\beta J} + 4368e^{-56\beta J} + 18748e^{-60\beta J}. \tag{D11}$$

Given the droplet partition functions, the droplet free energy $F(n)$ defined in this paper can be obtained from the following equation,

$$e^{-\beta F(n)} = \frac{\Omega_n}{1 + \sum_{i=1}^{\infty} \Omega_i}. \tag{D12}$$

Numerically, the summation in the denominator converges very quickly after summing over 2 to 3 terms. As an approximation, we may write $F(n) \approx -k_B T \ln \Omega_n$. But this approximation is not invoked in Sec. IV.

The droplet free energy computed from Eq. (D12) is used to determine the constant term d in Eq. (6), by requiring that $F(n)$ from the two equations matches at a given $n=n_0$. In this work, we have always used $n_0=1$. Setting n_0 to larger values (as long as the analytic expression exists) does not change the numerical results appreciably. For example, consider the 2D Ising model at $k_B T=1.5$, $h=0$ and $J=1$. The free energy of a droplet of $n=1$ is $F(1) \approx 8$, whereas Eq. (9) predicts that $F(1)=2\sqrt{\pi\sigma_{\text{eff}}} \approx 4.3$. This means that a constant correction term $d \approx 3.7$ is needed.

[1] J. E. McDonald, Am. J. Phys. **30**, 870 (1962).
[2] F. F. Abraham, *Homogeneous Nucleation Theory* (Academic, New York, 1974).
[3] R. J. Speedy and C. A. Angell, J. Chem. Phys. **65**, 851 (1976); P. H. Poole, F. Sciortino, U. Essmann, and H. E. Stanley, Nature (London) **360**, 324 (1992).
[4] E. Mendez-Villuendas and R. K. Bowles, Phys. Rev. Lett. **98**, 185503 (2007).
[5] R. J. Young, *Introduction to Polymers* (CRC Press, New York, 1981).
[6] M. Gleiser and E. Kolb, Int. J. Mod. Phys. C **3**, 773 (1992).
[7] R. Becker and W. Döring, Ann. Phys. (N.Y.) **24**, 719 (1935).
[8] Ya. B. Zeldovich, Ann. Phys. (N.Y.) **18**, 1 (1943).
[9] J. Frenkel, *Kinetic Theory of Liquids* (Oxford University Press, Oxford, 1946).
[10] L. Farkas, Z. Phys. Chem. (Munich) **125**, 236 (1927).
[11] A. Laaksonen, V. Talanquer, and D. W. Oxtoby, Annu. Rev. Phys. Chem. **46**, 489 (1995).
[12] J. Lothe and G. Pound, J. Chem. Phys. **36**, 2080 (1962).
[13] J. W. Cahn and J. E. Hilliard, J. Chem. Phys. **31**, 688 (1959).
[14] J. S. Langer, Ann. Phys. (N.Y.) **41**, 108 (1967); Phys. Rev. Lett. **21**, 973 (1968); Ann. Phys. (N.Y.) **54**, 258 (1969).
[15] X. C. Zeng and D. W. Oxtoby, J. Chem. Phys. **94**, 4472 (1991).
[16] C. Valeriani, E. Sanz, and D. Frenkel, J. Chem. Phys. **122**, 194501 (2005).
[17] E. Sanz, C. Valeriani, T. Vissers, A. Fortini, M. E. Leunissen, A. van Blassderen, D. Frenkel, and M. Dijkstra, J. Phys.: Condens. Matter **20**, 494247 (2008).
[18] S. Auer and D. Frenkel, Annu. Rev. Phys. Chem. **55**, 333 (2004).
[19] P. G. Bolhuis, D. Chandler, C. Dellago, and P. L. Geissler, Annu. Rev. Phys. Chem. **53**, 291 (2002).
[20] P. A. Rikvold, H. Tomita, S. Miyashita, and S. W. Sides, Phys. Rev. E **49**, 5080 (1994).
[21] V. A. Shneidman, K. A. Jackson, and K. M. Beatty, J. Chem. Phys. **111**, 6932 (1999).
[22] D. Stauffer, A. Coniglio, and D. W. Heermann, Phys. Rev. Lett. **49**, 1299 (1982).
[23] M. Acharyya and D. Stauffer, Eur. Phys. J. B **5**, 571 (1998).
[24] K. Brendel, G. T. Barkema, and H. van Beijeren, Phys. Rev. E **71**, 031601 (2005).
[25] A. C. Pan and D. Chandler, J. Phys. Chem. B **108**, 19681 (2004).
[26] R. J. Allen, C. Valeriani, S. Tanase-Nicola, P. R. ten Wolde, and D. Frenkel, J. Chem. Phys. **129**, 134704 (2008).
[27] L. Maibaum, Phys. Rev. Lett. **101**, 256102 (2008).
[28] S. Wonczak, R. Strey, and D. Stauffer, J. Chem. Phys. **113**, 1976 (2000).
[29] D. W. Heermann, A. Coniglio, W. Klein, and D. Stauffer, J. Stat. Phys. **36**, 447 (1984).
[30] H. Vehkamaki and I. J. Ford, Phys. Rev. E **59**, 6483 (1999).
[31] S. Ryu and W. Cai, Phys. Rev. E **81**, 030601(R) (2010).
[32] R. J. Allen, D. Frenkel, and P. R. ten Wolde, J. Chem. Phys. **124**, 024102 (2006); **124**, 194111 (2006).
[33] M. Volmer and A. Weber, Z. Phys. Chem. (Munich) **119**, 227 (1926).
[34] N. J. Gunther, D. J. Wallace, and D. A. Nicole, J. Phys. A **13**, 1755 (1980).
[35] M. J. Lowe and D. J. Wallace, J. Phys. A **13**, L381 (1980).
[36] D. J. Wallace, in *Phase Transitions*, Proceedings of a Summer Institute, Cargese, Corsica, 1980, edited by M. Levy, J. C. Le Guillou, and J. Ziin-Justin (Plenum, New York, 1982), p. 423.
[37] C. C. A. Gunther, P. A. Rikvold, and M. A. Novotny, Physica A **212**, 194 (1994).
[38] G. Jacucci, A. Perini, and G. Martin, J. Phys. A **16**, 369 (1983).
[39] A. Perini, G. Jacucci, and G. Martin, Phys. Rev. B **29**, 2689 (1984).
[40] R. K. P. Zia and D. J. Wallace, Phys. Rev. B **31**, 1624 (1985).
[41] D. Stauffer and C. S. Kiang, Phys. Rev. Lett. **27**, 1783 (1971).
[42] C. K. Harris, J. Phys. A **17**, L143 (1984).
[43] R. K. P. Zia and J. E. Avron, Phys. Rev. B **25**, 2042 (1982).
[44] M. Hasenbusch and K. Pinn, Physica A **203**, 189 (1994).
[45] T. S. van Erp, D. Moroni, and P. G. Bolhuis, J. Chem. Phys. **118**, 7762 (2003).
[46] E. E. Borrero and F. A. Escobedo, J. Chem. Phys. **129**, 024115 (2008).
[47] D. Moroni, P. G. Bolhuis, and T. S. van Erp, J. Chem. Phys. **120**, 4055 (2004).
[48] See supplementary material at http://link.aps.org/supplemental/10.1103/PhysRevE.82.011603 for free energy curves for cluster sizes up to $n=1950$ in a wide temperature range.
[49] V. A. Shneidman and G. M. Nita, J. Chem. Phys. **121**, 11232 (2004).
[50] G. Wilemski, J. Chem. Phys. **103**, 1119 (1995).
[51] Here, the word "prefactor" means the factor in front of the exponential term.
[52] Crowding of droplets, or interaction among droplets, have been investigated by Pan and Chandler [25] using very high field up to $h=1.18J$. They have found for the 3D Ising model, even for fields up to $h\sim 0.8J$ at $k_BT=0.6T_c$, the critical nucleus size n_c obtained by umbrella sampling and the critical nucleus size n_k obtained by commitor distribution matches well, indicating the crowding effect is negligible. Because in this paper, we consider field values much lower than $0.8J$, the crowding effect should be very small, as also confirmed by our own data on the two critical sizes. Indeed, the population of up-spins is at most 4% for the highest temperature and highest field conditions considered in our study, and is usually less than 2%. The interaction among those sparse up-spins would not affect free energy significantly.
[53] $2\sqrt{\pi n}$ is the circumference of a circle with area n. However, a real droplet is not compact but consists of a mixture of up and down spins. The percentage of down-spins in the droplet as a function of T is also absorbed in $\sigma_{\text{eff}}(T)$.
[54] This is against the expected temperature dependence of τ due to suppression of shape fluctuation below the roughening temperature, see Sec. II A.
[55] Perini *et al.* [39] originally introduced the "ledge" term in order to improve the quality of the fit in the range of $n<19$. However, we found that fitting to the data in the range of $n<19$ will lead to large discrepancies in the range of $n>100$. Given that the droplet theory is supposed to work better in the continuum limit of large n, we believe the function should be fitted to data at large n.
[56] Eq. (30) also fits the data at non-zero h. However, the resulting $\sigma_{\text{eff}}^{\text{3D}}$ from the fit slightly increases with h. For example, $\sigma_{\text{eff}}^{\text{3D}}$ increase by about 3% as h changes from 0 to 0.5.